Published in final edited form as:
Magn Reson Med. 2009 January ; 61(1): 244–248. doi:10.1002/mrm.21751.

7 T Whole Body Imaging: Preliminary Results

J. Thomas Vaughan,
Radiology, Ctr. for Magnetic Resonance Research, Univ. of Minnesota, Minneapolis, MN

Carl J. Snyder,
Radiology, Ctr. for Magnetic Resonance Research, Univ. of Minnesota, Minneapolis, MN

Lance J. DelaBarre,
Radiology, Ctr. for Magnetic Resonance Research, Univ. of Minnesota, Minneapolis, MN

Patrick J. Bolan,
Radiology, Ctr. for Magnetic Resonance Research, Univ. of Minnesota, Minneapolis, MN

Jinfeng Tian,
Radiology, Ctr. for Magnetic Resonance Research, Univ. of Minnesota, Minneapolis, MN

Lizann Bolinger,
National Research Council, Winnipeg, MB, Canada

Gregor Adriany,
Radiology, Ctr. for Magnetic Resonance Research, Univ. of Minnesota, Minneapolis, MN

Peter Andersen,
Radiology, Ctr. for Magnetic Resonance Research, Univ. of Minnesota, Minneapolis, MN

John Strupp, and
Radiology, Ctr. for Magnetic Resonance Research, Univ. of Minnesota, Minneapolis, MN

Kamil Ugurbil
Radiology, Ctr. for Magnetic Resonance Research, Univ. of Minnesota, Minneapolis, MN

Abstract

The objective of this study was to investigate the feasibility of whole body imaging at 7 T. To achieve this objective, new technology and methods were developed. Radio frequency field distribution and specific absorption rate were first explored through numerical modeling. A body coil was then designed and built. Multi-channel transmit and receive coils were also developed and implemented. With this new technology in hand, an imaging survey of the “landscape” of the human body at 7 T was conducted. Cardiac imaging at 7 T appeared to be possible. The potential for breast imaging and spectroscopy was demonstrated. Preliminary results of the first human body imaging at 7 T suggest both promise and directions for further development.

Keywords

7 T Body MRI; 7 T Cardiac MRI; 7 T Breast MRI; 7 T Breast MRS

Corresponding author: Thomas Vaughan, CMRR, 2021 Sixth St. S.E., University of Minnesota, Minneapolis, MN 55455, tommy@cmrr.umn.edu, phone: 612-625-8823, fax: 612-626-2004.

Introduction

Whole body imaging and its clinical applications have been commercially developed for 3 T. Body imaging has been demonstrated in research applications to 4 T (1). Since the late 1990's, 7 T has been used for human head imaging (2,3). The major MRI system manufacturers are now supporting 7 T whole body MRI systems for head imaging only. Radio frequency (RF) field non-uniformities have been observed due to destructive interference patterns of the short radio wavelengths, (12 cm in brain tissue). These destructive interferences have presented significant challenges to image homogeneity, contrast uniformity, signal to noise ratio (SNR) contours, and specific absorption rate (SAR) distributions in the body at 300 MHz, the 7-tesla ^{1}H Larmor frequency. New methods such as transmit RF field (B_1^+) shimming are being developed to overcome these problems (4,5). Human brain images with unprecedented SNR, spatial and temporal resolution, contrast, and spectral resolution are being acquired at 7 T (6-11). The SAR is being minimized through optimization methods employing B_1^+ shimming from multi-channel transmit coils, thus facilitating safe and efficient RF power management as well. Many human body applications will benefit significantly from increased SNR and spectral resolution, if the body can indeed be imaged successfully at the highest field strengths available. This note reports the results of the first feasibility results of human body imaging and spectroscopy at 7 T.

Methods

Modeling

The RF field and SAR were modeled by the Finite Difference Time Domain (FDTD) method (Remcom, Inc., State College, PA), for the human body loaded coil at 7 T. The body model used was derived from the National Library of Medicine (NLM) Visual Human digital atlas whose segmented anatomy was adjusted to match the conductivity and permittivity of tissues at 300 MHz. This body coil was driven at four ports (45°, 135°, 225°, 315°) referenced to 0° at the bottom of the coil as shown in Figure 1a. The inner diameter of the coil measured 57.5 cm, the outer diameter is 62.5 cm, the length of the 32 resonant elements was 33 cm, and the length of the cylindrical cavity required to shield these elements from the gradients was 100 cm (Figure 2). The magnitude of the magnetic component of the RF electromagnetic field was designated as "B_1". The B_1 field generated in the coil was circularly polarized and the magnitude was uniform in the unloaded state.

Hardware Development

RF coils and drive circuits for human body imaging at 7 T were not commercially available, and therefore had to be developed for this investigation. The MRI system used for the study was built around a Magnex 7 T, 90 cm bore magnet (Magnex Scientific, Oxfordshire, UK) equipped with Magnex body gradients and a Symphony gradient amplifier (Siemens, Erlangen, Germany). Interfaced to this magnet was a Unity Inova spectrometer (Varian, Palo Alto, CA), together with a custom, 8 kW solid-state RF power amplifier (Communications Power Corporation (CPC), Hauppauge, NY). The whole body images in this report were acquired with an actively detuneable 300 MHz transverse electromagnetic (TEM) body coil shown in Figure 1b, built to the dimensions used in the computer modeling (1). Also developed was an eight channel TEM surface coil shown in Figures 1c,d. For imaging the human trunk, these surface coils were used in pairs, located anterior and posterior to the region of interest in the body. The elements of these multi-channel, transmit and receive coils were driven independently from a new 16 channel, parallel transceiver designed in-house and built by CPC (5,12). This system enabled RF transmit phase and magnitude control of each of the coil array's 16 independent elements to facilitate B_1^+ shimming and

parallel imaging methods (1,5,7,13-17). The term B_1^+ refers to the transmit component of the RF magnetic field vector, in contrast to the RF receive field (B_1^-). A circularly-polarized, unilateral RF breast coil consisting of two shielded crossed loops was also built and tested, presented later in Figure 5a (18).

Data Acquisition

Body Imaging with TEM Body Coil—The abdomen and thorax of a healthy normal, adult human were imaged with the body coil, in an institutional review board approved study at 7 T. Due to the limited peak power available (approximately 4 kW at the coil) and the signficant high-frequency load losses predicted, the initial experiments employed low flip angle sequences of greater pulse widths. For an initial mapping of the RF "landscape" in the body at 300 MHz, coronal, sagittal, and transaxial images were acquired with the body coil switched to transmit and receive mode, without the use of additional receiver coils. The receive signal was acquired by one of two methods: analog, quatrature phased recombination as shown in Figure 1a, or sum-of-squares combination from four individually received ports. The common parameters used for acquiring the gradient echo, whole body images of Figures 3 and 4a were: 256×256 matrix, 3 mm thick slice, 2 ms windowed 3-lobed sinc RF pulse, nominal flip angle = 25°. Specific to the coronal images: repetition time / echo time (TR/TE) = 60/4 ms, field of view (FOV) = 50×35 cm, number of excitations (NEX) = 4, scan time = 110 s. The sagittal images were acquired by: TR/TE = 50/4 ms, FOV = 50×35 cm, NEX = 2, scan time 55 s, and the transaxial images required: TR/TE = 50/4 ms, FOV = 35×35 cm, NEX = 4, scan time 110 s.

Body Imaging with Multi-channel TEM Surface Coil—Employing multi-channel transceiver coils closely fitted to the body offers an alternative to whole body coils for imaging localized regions of interest. Each element in the transceiver array was driven by a dedicated RF power amplifier with independent phase and magnitude control, a transmit/receive switch, and a pre-amplifier for reception. RF power was monitored for each channel. In the cardiac imaging example shown in Figures 4b, c, low flip angle, breath held, electrocardiogram retro-gated, gradient echo images were acquired using the parameters: TR/TE = 30/3.0 ms; matrix size = 144 × 192; 2.0 × 2.0 × 5.0 mm resolution (4b); 1.7 × 1.7 × 5.0 mm resolution (4c). These 7 T cardiac images were acquired with an Avanto body gradient interfaced to a Siemens spectrometer, a later upgrade to the 7T system described. To mitigate RF artifacts and to maximize excitation efficiency (reducing SAR), B_1^+ shimming was applied. The relative transmit B_1^+ phases of the coil elements were calculated and established by acquiring phase maps (4,19) to determine a set of transmit phases required to maximize the B_1^+ phase coherence within a given region of interest.

Breast Imaging and Spectroscopy with Quadrature Surface Coil—MRI and MRS data were acquired from a healthy normal female volunteer using the transmit/receive surface coil of Figure 5a. To distinguish fibro-glandular from adipose tissue, T_1-weighted images were acquired using a fat-suppressed 3D gradient-recalled echo sequence. Acquisition parameters were: TR/TE = 15/5 ms, FOV = 14 cm × 14 cm × 14 cm, and matrix = 256×256×64. Single-voxel spectra were collected using the LASER pulse sequence (20) and echo time averaging. To quantify fibro-glandular choline-containing compounds, the unsuppressed water signal in the voxel was used as an internal reference. The LASER single voxel spectroscopy was preformed with a 1.6 mL voxel, TR=3 s, TE=43-195 ms in 128 increments, and processed with 8 Hz line broadening.

Results and Discussion

7 T Models

Results from numerical calculations of the B_1 and SAR contours in the NLM human male at 300 MHz are shown in Figure 2. Figures 2a, b, show the calculated B_1 distribution in a loaded body coil for this frequency. Interference patterns are shown to create the non-uniformities in the B_1 field within and outside of the body at 7 T. In the body, these nonuniformities span 40 dB, with the lowest level B_1 regions running longitudinally in the body center, and the highest B_1 magnitudes in the periphery of the body near the four driven elements. Interestingly, the head located well outside of the coil elements, experiences some of the highest B_1 values. The central blue colored lines of RF destructive interference in the Figure 2 a,b, models are observed as dark lines in the body images of Figure 3. Figures 2c,d show the calculated SAR distribution in the body excited by the 300 MHz body coil described. The SAR contours span a 50 dB gradient, with maximum SAR experienced in the tissues nearest the drive elements of the coil, and the lowest SAR values found near the center-line of the body. The severe B_1 and SAR gradients modeled suggest that conventional MRI methods employing a homogeneous, circularly polarized body coil for uniform excitation of the body may not be possible for whole body, ^{1}H imaging at 7 T. B_1^+ shimming with a body coil may however offer a solution.

7 T MRI with Body Coil

The results of the 3D electromagnetic model of a human in a 7 T body coil predicted significant RF artifacts running longitudinally through the center of the body due to destructive interference of the short (12 cm) wavelengths at 300 MHz due to the high dielectric constants of high water-content tissues. Initial images appear to follow these predictions. Central dark bands seen in the abdominal images of Figure 3 could not be excited within U.S. Food and Drug Administration (FDA) SAR guidelines. The RF power (SAR) used to acquire the images presented was 11.1 W per slice. For the five interleaved slices, the total power used to acquire these first data sets was 55.5 W, less than 1 W/kg for the 80 kg subject imaged and well within the FDA guidelines for human torso imaging. Initial images of the human thorax in Figure 4 however, show some promise for cardiac imaging. The longer wavelengths in the low density lung tissue of the chest may improve the B_1^+ penetration to the pericardium. It was found that receiving the signal from the four independent channels of the body coil, and constructing images by simple sum-of-squares magnitude addition resulted in images with 20% more SNR than images acquired by circularly phased analog recombination of the received signal.

7 T Body Imaging with Multi-channel TEM Surface Coil

Not all “body” imaging is best served with a body coil. Cardiac imaging and spectroscopy can benefit greatly from the temporal, spatial, and spectral resolution inherent to 7 T. Compared to the body coil results in Figure 4a, significant improvements in heart image SNR and B_1^+ uniformity were achieved by using the multi-channel transceiver of Figure 1d, together with B_1^+ shimming. This improvement is evident in the four-chamber (Figure 4b) and short axis (Figure 4c) views acquired with the multi-channel surface coil. The local SAR required for these improved surface coil images was approximately the same 1 W/kg used to acquire the body images. Use of local, multi-channel, transceiver coils with B_1^+ shimming has proven successful in 7 T prostate imaging as well (19).

7 T MRI and MRS with Local Transmit and Receive Coil

For local imaging and spectroscopy of more superficial anatomy such as the breasts, conventional transceiver surface coils can be used effectively. Early results from a 7 T breast

cancer study give examples of the promise of 7 T diagnostics (18). Measurement of total choline-containing compounds (tCho) by localized ^{1}H MRS offers a means to distinguish malignant from benign lesions and to predict response to neoadjuvant chemotherapy. The detection of tCho in small lesions having low cellularity is usually limited by insufficient SNR at clinical field strengths. Previous breast MRS studies at 4 T have reported higher SNR, enabling the detection of tCho in smaller lesions as well as the occasional detection of other metabolites such as taurine, creatine, and glycine (21). The ability to detect relatively narrow tCho and taurine resonances in normal breasts shown in Figure 5b, c, provides motivation to investigate breast cancer at 7T.

Conclusions

First examples of theoretical models, technology and methods for investigating the feasibility of 7 T body imaging have been demonstrated. Technology developments include a 300 MHz body coil, a multi-channel surface coil, and a small, quadrature surface coil. Preliminary imaging results show whole body imaging at 7 T with a body coil, and with locally placed multi-channel transceiver coils and B_1^+ shimming. Models and measurements indicate that the conventional, uniform, circularly polarized body coil may have limitations for homogeneous excitation at 7 T. Locally placed, multi-channel transceivers could provide a solution to body coil shortcomings at 7 T. Improvements in both signal intensity and homogeneity appear to be gained when using multi-channel transceiver coils with B_1^+ shimming for imaging local regions of interest. Local, single channel or quadrature surface coils may also be useful, especially for superficial regions of interest. Cardiac and breast imaging and spectroscopy appear to be early applications worth pursing at 7 T. With the proper selection of coils and methods such as B_1^+ shimming, general body imaging appears to be feasible at 7 T.

Acknowledgments

NIH-R33 CA94318, NIH-R01 CA94200-01A1, NIH-R01 EB000895-04, NIH-P41 RR08079

References

1. Vaughan J, Adriany G, Snyder C, Tian J, Thiel T, Bolinger L, Liu H, DelaBarre L, Ugurbil K. Efficient high-frequency body coil for high-field MRI. Magn Reson Med. 2004; 52:851–859. [PubMed: 15389967]
2. Vaughan J, Garwood M, Collins C, DelaBarre L, Adriany G, Andersen P, Merkle H, Smith M, Ugurbil K. 7T vs. 4T: RF power, homogeneity & signal-to-noise comparison in head images. Magn Reson Med. 2001; 46:24–30. [PubMed: 11443707]
3. Yacoub E, Shmuel A, Pfeuffer J, Van de Moortele PF, Adriany G, Andersen P, Vaughan JT, Merkle H, Ugurbil K, Hu XP. Imaging brain function in humans at 7 Tesla. Magnetic Resonance in Medicine. 2001; 45(4):588–594. [PubMed: 11283986]
4. Van de Moortele PF, Akgun C, Adriany G, Moeller S, Ritter J, Collins C, Smith M, Vaughan J, Ugurbil K. B_1 destructive interferences and spatial phase patterns at 7 tesla with a head transceiver array coil. Magn Reson Med. 2005; 54(6):1503–1518. [PubMed: 16270333]
5. Vaughan J, DelaBarre L, Snyder C, Tian J, Akgun C, Shrivastava D, Olson C, Adriany G, Liu W, Strupp J, Andersen P, Gopinath A, Van de Moortele PF, Garwood M, Ugurbil K. 9.4T Human MRI: Preliminary Results. Magn Reson Med. 2006; 56:1274–1282. [PubMed: 17075852]
6. Moeller S, Van de Moortele PF, Goerke U, Adriany G, Ugurbil K. Applicatoin of parallel imaging to fMRI at 7 tesla utilizing a high 1D reduction factor. Magn Reson Med. 2006; 56:118–129. [PubMed: 16767760]
7. Adriany G, Van de Moortele PF, Wiesinger F, Moeller S, Strupp J, Andersen P, Snyder C, Zhang X, Chen W, Pruessmann K, Boesiger P, Vaughan J, Ugurbil K. Transmit and receive transmission line

arrays for 7 tesla parallel imaging. Magnetic Resonance in Medicine. 2005; 53(2):434–445. [PubMed: 15678527]

8. Yacoub E, Van de Moortele PF, Schmuel A, Ugurbil K. Signal and noise characteristics of Hahn SE and GE BOLD fMRI at 7T in humans. Neuroimage. 2005; 24:738–750. [PubMed: 15652309]
9. Qiao H, Zhang X, Zhu XH, Du F, Chen W. In vivo ^{31}P MRS of human brain at high/ultrahigh fields: a quantitative comparison of NMR detection sensitivity and spectral resolution between 4T and 7T. Magn Reson Imag. 2006; 24:1281–1286.
10. Mangia S, Tkac I, Gruetter R, Van de Moortele PF, Giove F, Maraviglia B, Ugurbil K. Sensitivity of single-voxel ^{1}H-MRS in investigating the metabolism of the activated human visual cortex at 7T. Magn Reson Imag. 2006; 24:343–348.
11. Li T, van Gelderen P, Merkle H, Talagala L, Koretsky A, Duyn J. Extensive heterogeneity in white matter intensity in high-resolution T_2^*-weighted MRI of the human brain at 7.0T. Neuroimage. 2006; 32(3):1032–1040. [PubMed: 16854600]
12. Vaughan, J.; Adriany, G.; Ugurbil, K.; Strupp, J.; Andersen, P.; University of Minnesota, assignee. Parallel Transceiver for Nuclear Magnetic Resonance System. USA patent 6,969,992. 2005.
13. Vaughan J, Hetherington H, Otu J, Pan J, Pohost G. High frequency volume coils for clinical nuclear magnetic resonance imaging and spectroscopy. Magn Reson Med. 1994; 32:206–218. [PubMed: 7968443]
14. Vaughan, J.; Massachusetts General Hospital, assignee. RF coil for imaging system. USA patent 6,633,161. 2003.
15. Vaughan, J.; Adriany, G.; Ugurbil, K.; Univeristy of Minnesota, assignee. Shim, gradient, and parallel imaging coil. USA patent 7,268,554 USA. 2003.
16. Wiesinger F, Van De Moortele PF, Adriany G, De Zanche N, Ugurbil K, Pruessmann KP. Parallel imaging performance as a function of field strength - An experimental investigation using electrodynamic scaling. Magnetic Resonance in Medicine. 2004; 52(5):953–964. [PubMed: 15508167]
17. Vaughan T, DelaBarre L, Snyder C, Tian J, Bolan P, Garwood M, Adriany G, Strupp J, Andersen P, Van de Moortele PF, Ugurbil K. Highest field human MR imaging. IEEE Transactions on EMC. 2006:213.
18. Vaughan J, Snyder C, DelaBarre L, Bolinger L, Tian J, Andersen P, Strupp J, Adriany G, Ugurbil K. 7T Body Imaging: First Results. 2006:213.
19. Metzger GJ, Snyder C, Akgun C, Vaughan T, Ugurbil K, Van de Moortele PF. Local B_1^+ shimming for prostate imaging with transceiver arrays at 7T based on subject-dependent transmit phase measurements. Magn Reson Med. 2008; 59(2):396–409. [PubMed: 18228604]
20. Garwood M, DelaBarre L. The return of the frequency sweep: Designing adiabatic pulses for contemporary NMR. Journal of Magnetic Resonance. 2001; 153(2):155–177. [PubMed: 11740891]
21. Haddadin IS, McIntosh A, Meisamy S, Corum C, Snyder AL, Powell NJ, Nelson MT, Yee D, Garwood M, Bolan PJ. Metabolite quantification and high-field MRS in breast cancer. NMR Biomed. 2008

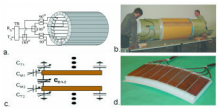

Figure 1.
7 T TEM body and surface coils (14). Figure 1a. shows a schematic diagram of the TEM body coil connected for four-port transmit and receive (1). Figure 1b shows the body coil mounted on the Siemens bore tube for insertion into the Siemens Sonata gradients. The transmission line "rungs" of the coil occupy the middle third (33 cm) of the one-meter coil as shown. The cavity or shield component of the coil is slotted for gradient induced eddy current attenuation and TEM element segregation. Figure 1c shows a schematic of a section of the TEM surface coil. The capacitances C_T, C_M, and C_D are for tuning, matching, and decoupling the independent elements respectively. Figure 1d shows an eight element TEM surface coil (32 cm × 15 cm) built of eight sets of two parallel copper strips separted by a 2 cm thick polytetrafluoroethylene dielectric, with eight independent drive cables connected.

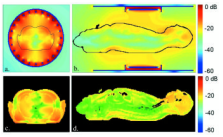

Figure 2.
Finite difference time domain models of B_1 and SAR contours generated by a body coil in the human body at 7 T. Figures 2a and 2b show relative B_1 magnitude isocontours, T/m (dB) in centerline transverse and sagittal planes. Figures 2c and 2d show SAR, W/kg (dB) isocontours in the same planes, respectively.

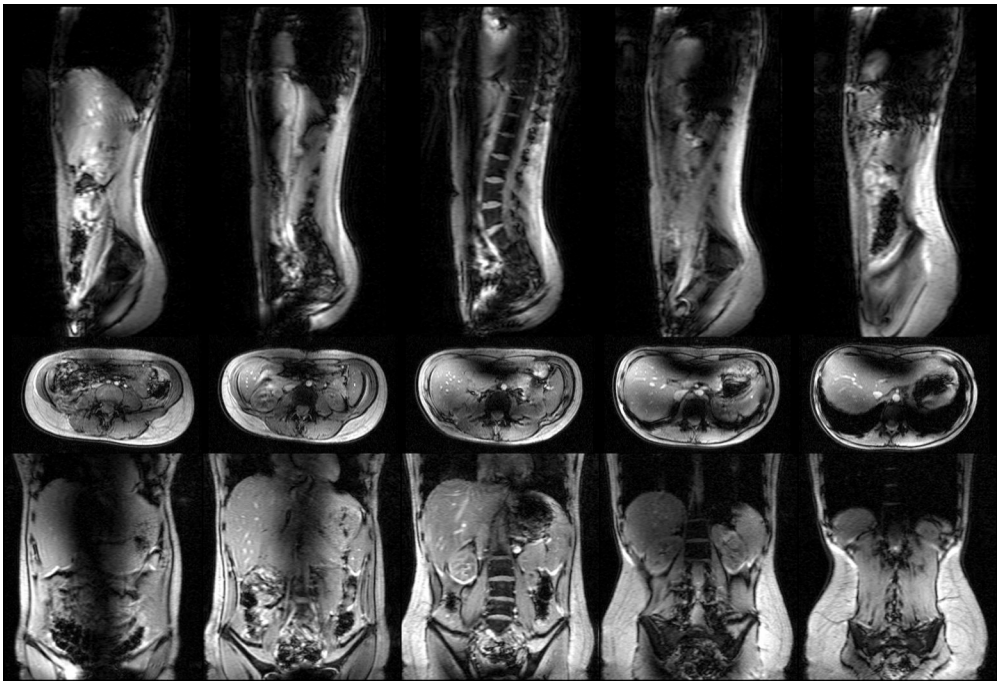

Figure 3.
Whole body abdominal images at 7 T. The coronal, sagittal, and transaxial, multi-slice image sets were acquired with body coil transmit and receive using low-tip, low power, low resolution gradient echo sequences. No intensity correction has been applied to the data.

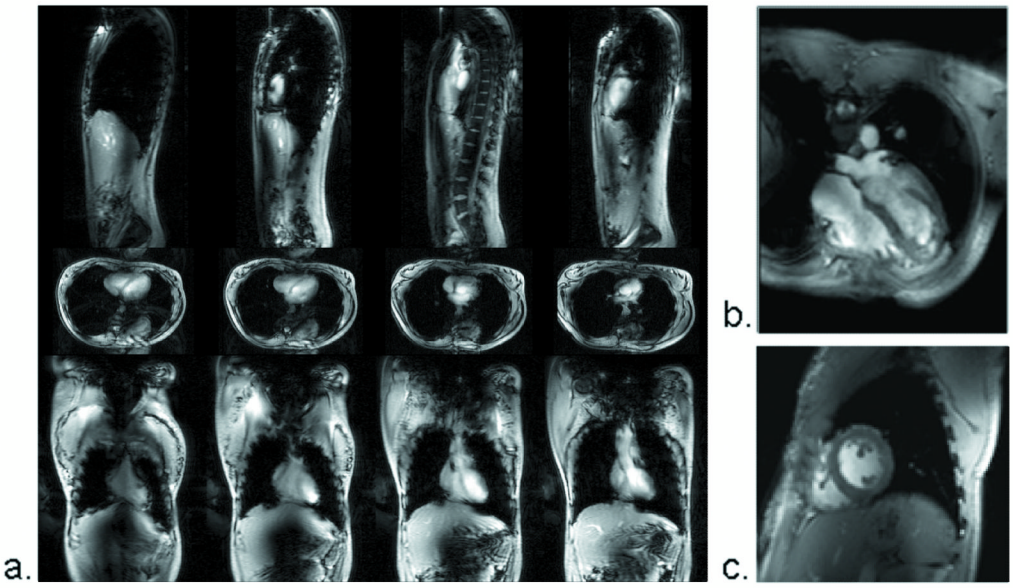

Figure 4.
Whole body thorax images at 7 T. Using the same imaging parameters as in Figure 4, the heart is visible in coronal, sagittal and transaxial, multi-slice planes.

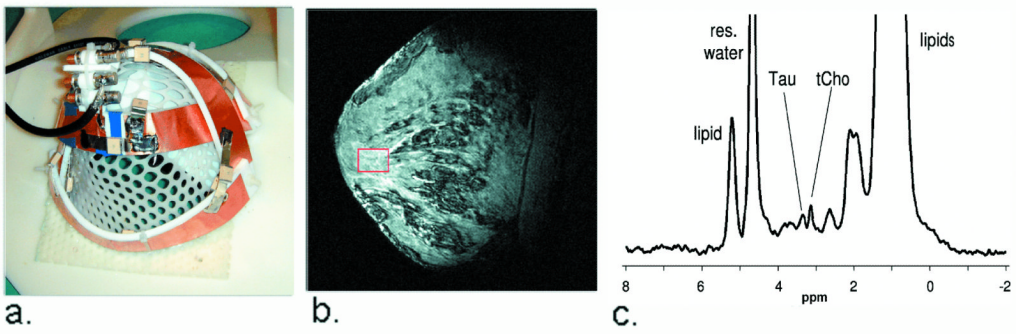

Figure 5.

Breast imaging and spectroscopy at 7 T. Figure 5a shows a crossed-pair surface coil transceiver used to acquire breast images (5b), and proton spectra (5c). Figure 5b shows a sagittal slice from a fat-suppressed, T_1-weighted 3D FLASH image acquired in a normal subject. The box indicates voxel placement in the fibro-glandular tissue. A single voxel spectrum acquired from the voxel indicated in 5b appears in 5c. Peaks from taurine and total choline are visible.